Group Identification in N-Body Simulations: SKID and DENMAX Versus Friends-of-Friends*

Martin Götz^{†‡§}, John P. Huchra[†], Robert H. Brandenberger[‡]
April 17, 2018

Abstract

Three popular algorithms (FOF, DENMAX, and SKID) to identify halos in cosmological N-body simulations are compared with each other and with the predicted mass function from Press-Schechter theory. It is shown that the resulting distribution of halo masses strongly depends upon the choice of free parameters in the three algorithms, and therefore much care in their choice is needed. For many parameter values, DENMAX and SKID have the tendency to include in the halos particles at large distances from the halo center with low peculiar velocities. FOF does not suffer from this problem, and its mass distribution furthermore is reproduced well by the prediction from Press-Schechter theory.

1. Introduction

N-body simulations are a frequently used tool in cosmology to study the origin of large-scale structure in the universe or the formation of galaxies. For these applications, it is necessary to identify the dark matter halos in the models, as those are interpreted to be the locations of galaxies or galaxy clusters. Ideally, the way in which the dark matter halos are extracted should not influence the results sought in the simulations, e.g. the mass distribution, correlation function, formation and merging rates, and many other properties of the halos. Fortunately or unfortunately, many different algorithms to identify groups of particles in N-body simulations have been proposed. The question we address here is how the choice of algorithm affects the properties of halos.

The attention of the authors was drawn to this

question by the results shown in Fig. 1. shows the mass distribution of halos, in the form of the differential mass function, at redshift z =0 for a series of N-body simulations, run with a particle-particle/particle-mesh (P³M) code by E. Bertschinger and J. M. Gelb [1]. The simulations, originally carried out for a different purpose, are of a standard cold dark matter (SCDM) model ($\Omega_0 = 1$ and $H_0 = 50 \text{ km/s/Mpc}$) with 64^3 particles in boxes of sizes varying from 50 Mpc to 1600 Mpc. The mass distribution of halos was determined in two different ways, using two popular algorithms: friends-offriends (FOF), a percolation algorithm, and DEN-MAX. (See below for a description of how these algorithms work.) Fig. 1 reveals that the two algorithms give very different results for the number of massive halos in large simulations. In particular, DEN-MAX overpredicts their number when compared to FOF or the theoretical prediction based upon Press-Schechter theory. (Again, see below for an explanation of Press-Schechter theory.) Thus the choice of group identification algorithm indeed has an effect on the properties of halos, and this article attempts to explore this by comparing three of the more popular algorithms.

Section 2 gives a brief overview of the N-body simulations used to provide the 'raw material' for the comparison. Section 3 introduces the three different algorithms which had been chosen for that purpose. Section 4 describes Press-Schechter theory, which is used as a baseline to compare the mass distribution of halos as identified by the different algorithms, and how the agreement (or disagreement) with Press-Schechter theory can be quantified. The next section contains the actual results of the comparisons, how these depend upon the choice of the free parameters in the algorithms, the box sizes of the simulation, and the cosmology. This is then followed by the conclusions.

^{*}Preprint BROWN HET-1140

 $^{^\}dagger Harvard\text{-}Smithsonian$ Center for Astrophysics, 60 Garden St., MS-20, Cambridge, MA 02138

 $^{^{\}ddagger} \text{Physics}$ Department, Brown University, Box 1843, Providence, RI 02912

[§]To whom communication should be addressed. E-mail: mgotz@cfa.harvard.edu

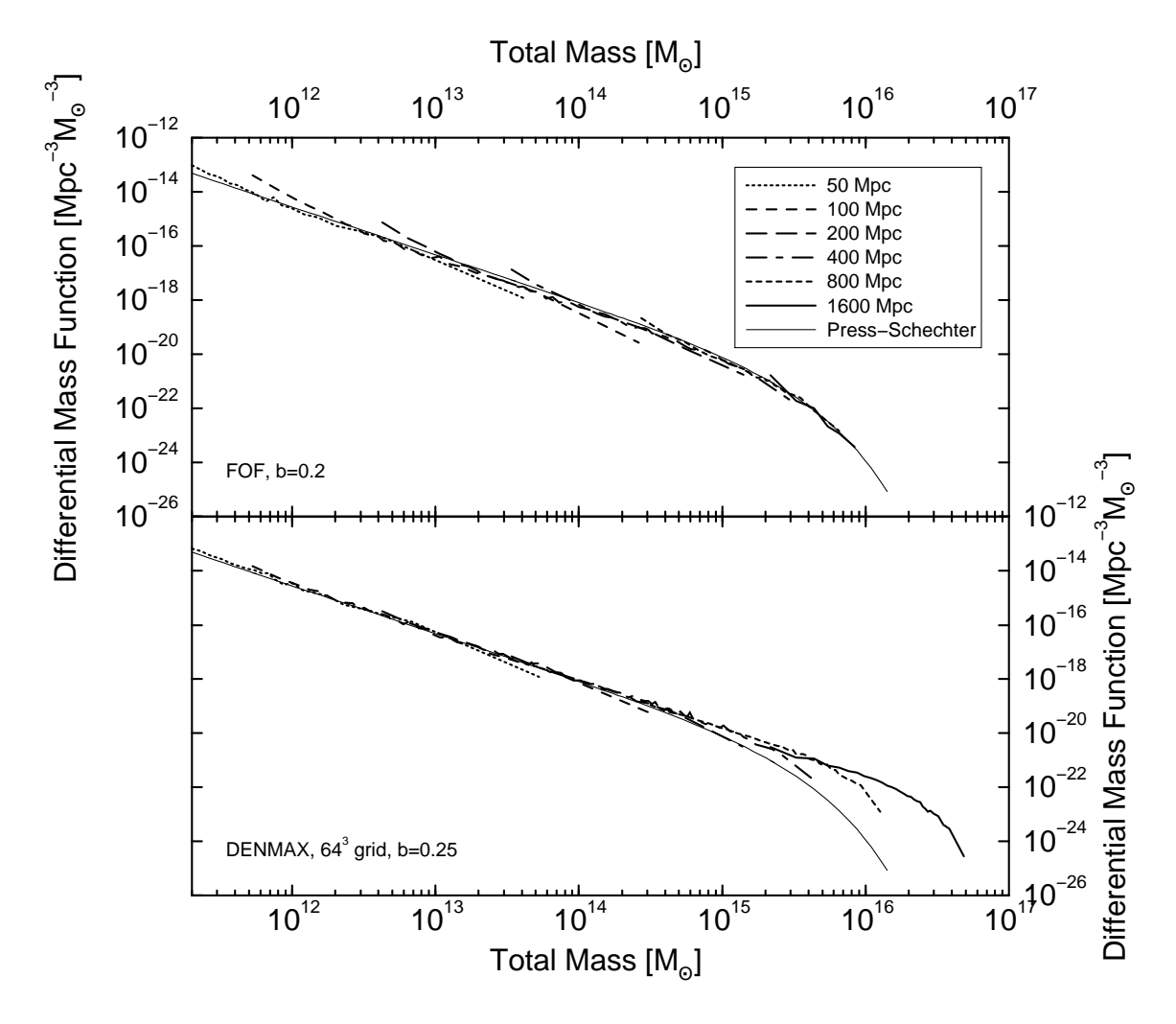


Figure 1: The differential mass functions of halos for a series of N-body simulations in an SCDM scenario $(\Omega_0 = 1, h = 0.5)$ at redshift z = 0, run with the P³M code from [1], for varying box sizes, but with 64^3 particles each. Groups were identified with two popular algorithms: friends-of-friends (FOF) and DENMAX. Both have as a free parameter a linking length between neighboring particles b, here given in units of the mean particle separation. In addition, DENMAX has as a second parameter the size of the grid on which the densities of particles are calculated, chosen to be the same size as the number of particles here. Compared to FOF or a theoretical prediction from Press-Schechter theory, DENMAX produces more massive halos in large simulations.

2. The Simulations

To test the reliability of group identification algorithms we use representative results of N-body simulations. The first indications of the effects of different group identification algorithms were found in N-body simulations with the P³M code by E. Bertschinger and J. M. Gelb [1]. We decided to use a different code for this systematic study. The simulations were run with the Hydra code by H. M. P. Couchman et al. [2]. Hydra incorporates the evolution of both, dark matter via

an adaptive particle-particle/particle-mesh method (AP³M), and of baryonic gas with smoothed particle hydrodynamics (SPH). It was run with dark matter particles only since the goal was to provide typical cosmological settings for halo identification. Hydra was chosen because of its higher computational efficiency in high density regions, which are the regions we are particularly interested in, and because software to identify groups in the output files produced by Hydra is readily available. Two "favorite" cosmological scenarios were chosen: an open cold dark matter model (OCDM) with $\Omega_0 = 0.4$, a

Simulation		Ω_0	h	σ_8	# of	soft.	$z_{ m initial}$	# of
					part.	length		steps
OCDM,	$50 \; \mathrm{Mpc}$	0.4	0.6	0.8	64^{3}	0.1	199	2022
	$100~{ m Mpc}$	0.4	0.6	0.8	64^{3}	0.1	199	1333
	$200~\mathrm{Mpc}$	0.4	0.6	0.8	64^{3}	0.1	199	681
	$400~{ m Mpc}$	0.4	0.6	0.8	64^{3}	0.1	199	337
	$800~\mathrm{Mpc}$	0.4	0.6	0.8	64^{3}	0.1	199	163
	$1600\;\mathrm{Mpc}$	0.4	0.6	0.8	64^{3}	0.1	199	92
SCDM,	$50 \; \mathrm{Mpc}$	1.0	0.5	1.0	64^{3}	0.1	199	2865
	$100~{ m Mpc}$	1.0	0.5	1.0	64^{3}	0.1	199	1880
	$200~\mathrm{Mpc}$	1.0	0.5	1.0	64^{3}	0.1	199	999
	$400~{ m Mpc}$	1.0	0.5	1.0	64^{3}	0.1	199	459
	$800~\mathrm{Mpc}$	1.0	0.5	1.0	64^{3}	0.1	199	215
	$1600\;\mathrm{Mpc}$	1.0	0.5	1.0	64^{3}	0.1	199	104

Table 1: Parameters of the OCDM and SCDM simulations with varying box sizes used in comparing the different group identification algorithms. h is the Hubble constant in units of 100 km/s/Mpc. The gravitational softening length is given as a fraction of the mean particle separation, and is kept constant in comoving coordinates during the simulation. The value corresponds to that of an equivalent Plummer softening length, although the Hydra code uses a slightly different shape [2]. Timestepping is regulated automatically by the code, and the number of steps, which may not be of equal length, necessary to reach redshift zero is given in the last column.

Hubble constant of $H_0=60~{\rm km/s/Mpc}$, normalized in such a way that $\sigma_8=0.8$ at present time, consistent with the observed abundance of galaxy clusters [3, 4]. The second model was standard cold dark matter (SCDM) with $\Omega_0=1,\,H_0=50~{\rm km/s/Mpc}$, and $\sigma_8=1$. For each model, simulations were run with 64^3 particles with box sizes varying from 50 Mpc to 1600 Mpc in steps of a factor of two both to insure a wide dynamic range in the masses of the dark matter halos and to see at which resolution the group identification algorithms break down. Table 1 lists all the parameters of the simulations, including the gravitational softening employed, initial redshift, and the number of timesteps.

3. Identifying Groups

At redshift zero, groups in the distribution of dark matter particles were identified using three common algorithms: the friends-of-friends (FOF) method, DENMAX, and SKID. With FOF [5, 6], particles are joined into groups if the separation to the nearest neighbor is less than a given threshold, called the linking length b, which is the only free parameter for this algorithm. We will express b in units of the mean particle separation throughout this paper. Then $1/b^3$ corresponds to an overdensity, and FOF approximately groups together particles which lie inside the corresponding level surfaces.

Group identification in DENMAX [1, 7] and SKID

[8, 9] is a three-step process. First, particles are moved in small steps in the direction of the local density gradient, until their locations stay within a small distance, the convergence radius, for a certain number of steps, which means that they oscillate around a local density maximum. In the second step, groups among the particles at their moved positions are identified with a FOF algorithm with a linking length b twice the convergence radius. The third and last step then removes particles which are not gravitationally bound to the groups identified in the previous step. This is done by calculating the potential energies of all of the particles in the group (now at their original, unmoved locations) and their kinetic energies (with peculiar velocities with respect to the center of mass of the group and an additional velocity due to the Hubble expansion of the halo). If there are unbound particles with positive total energy, the one with the highest total energy is removed from the group, and the process of calculating potential and kinetic energies is repeated, until there are no unbound particles left. Note that this implementation of DENMAX actually follows SKID and is slightly different from the originally proposed [1, 7]. The difference between DENMAX and SKID lies in the way densities, and thus their gradients, are determined in the first step. For DENMAX, they were calculated on a fixed grid with a triangular shaped cloud (TSC) scheme [10, Ch. 5-3-2], the same as in the P³M code. SKID instead uses a symmetric SPH smoothing kernel [11] considering a certain number of neighbors around each particle to smooth over. Hence the main difference between the two algorithms is that DENMAX computes density gradients on a fixed Eulerian scale, whereas SKID computes them on a fixed Lagrangian scale, adjusting the resolution of this calculation to the local density. Different to FOF, DENMAX and SKID have two free parameters each: the linking length b and the size of the grid (for DENMAX) or the number of nearest neighbors (for SKID) used in calculating the density gradients.

4. Press-Schechter Theory and How to Compare With It

One of the most basic quantities derived from identifying halos is the distribution of their masses, which should be insensitive to different algorithms. To this end, the differential mass function n(M), i.e. the number density of halos with masses between M and $M+\mathrm{d} M$ as obtained in the simulations and by the different algorithms, was compared with the prediction from Press-Schechter theory [12, 13] based upon the power spectrum P(k) used for the initial conditions in the simulations

$$n_{\rm PS}(M) \, dM = -\sqrt{\frac{2}{\pi}} \frac{\bar{\rho}}{M^2} \frac{\delta_c}{D\sigma(M)} \frac{d \ln \sigma}{d \ln M} \exp\left[-\frac{\delta_c^2}{2D^2 \sigma^2(M)}\right] dM.$$
 (1)

We use the form of the differential mass function as given by [14] for redshift z=0, the case we are interested in. $\bar{\rho}$ is the present mean mass density of the universe, $\delta_{\rm c}$ the linearly extrapolated overdensity at which a top-hat shaped overdensity has collapsed ($\delta_{\rm c}=1.686$ for SCDM and $\delta_{\rm c}=1.660$ for OCDM at z=0—see [15] for a discussion of this quantity and its dependence upon cosmological parameters and redshift). σ is the fractional r.m.s. mass fluctuation within a top-hat of radius R in the initial conditions of the simulation

$$\sigma^2(R) = 4\pi \int_0^\infty k^2 \mathrm{d}k \ P(k) W_R^2(k),$$

where $W_R(k)$ is the Fourier transform of the top-hat window function

$$W_R(k) = 3\left[\frac{\sin kR}{(kR)^3} - \frac{\cos kR}{(kR)^2}\right].$$

The connection between σ as a function of radius and sigma as a function of mass, which is needed in evaluating eq. (1), is then

$$M = \frac{4\pi}{3}R^3\bar{\rho},$$

via the average mass contained within the top hat. Finally, D in eq. (1) is the ratio of the growing modes of linear perturbation theory D(z) at present time and at the redshift of the initial conditions $D = D(z=0)/D(z=z_{\rm initial})$.

In the interpretation and derivation of [13, 14], the Press-Schechter prediction (1) gives the mass distribution of regions which lie inside contours with density contrast δ_c , which is the linearly extrapolated density contrast at which a full calculation, which is possible for a top-hat shaped overdensity, shows that the region has already collapsed.

Since one of the group identification algorithms (FOF) showed a good agreement with Press-Schechter theory in the simulations which drew our attention to this problem (Fig. 1), we decided to use Press-Schechter theory as a baseline for comparing the different algorithms. To quantify the differences in the differential mass functions obtained in the simulations, n(M), and from Press-Schechter theory, $n_{PS}(M)$, we simply integrate the difference squared between appropriate masses M_0 and M_1 to obtain a goodness of agreement Δ

$$\Delta = \int_{\lg M_0}^{\lg M_1} \left[\lg n(M) - \lg n_{PS}(M) \right]^2 \, d\lg M, \quad (2)$$

but with the logarithms taken of all relevant quantities. (Here, we use logarithms to base 10 and express the differential mass functions in units of ${\rm Mpc^{-3}}M_{\odot}^{-1}$ and masses in M_{\odot} .) Since the differential mass functions approximately drop as a power law with increasing mass, introducing the logarithms in (2) assures that differences at the low-mass end contribute as much to Δ as differences at the high-mass end.

5. Results

The three different group finding algorithms, with varying parameters, were applied to the results of the N-body simulations, and the resulting differential mass functions of halos were compared with Press-Schechter theory. First, we looked at how the parameters of the algorithms influence the mass function, and then how varying the box size of the simulation (and thus effectively changing the resolution of the halos) affected the results.

5.1. Varying the Parameters

Fig. 2 represents the differential mass functions in a typical case, here a $400~\rm Mpc$ box with $64^3~\rm particles$ from the series of OCDM Hydra simulations.

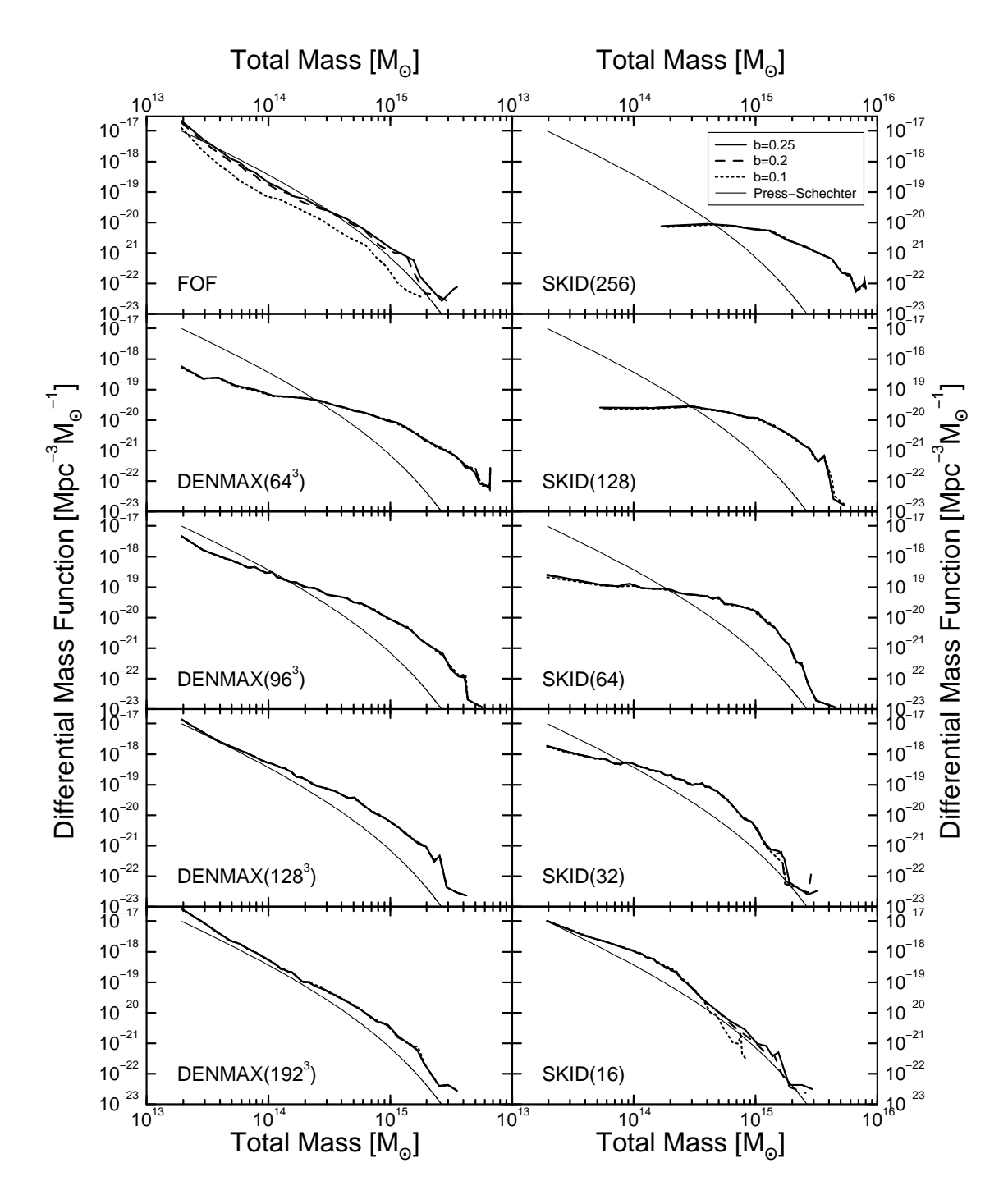


Figure 2: The differential mass functions obtained by different group finding algorithms and how they vary with their parameters. The halos were all identified at redshift z=0 of the same OCDM simulation $(\Omega_0=0.4,\,h=0.6)$ run with Hydra using 64^3 dark matter particles in a 400 Mpc box. The linking length b, a variable in all of the three algorithms, is given in units of the mean particle separation. In addition to b, DENMAX and SKID have as additional parameters the grid size or the number of nearest neighbors used to calculate the density gradients, respectively. These numbers are given in parentheses. Note that for DENMAX and SKID the differential mass function barely depends upon the linking length, contrary to FOF. The differential mass function predicted from Press-Schechter theory is plotted as a thin line in all of the graphs as a comparison. The scatter at the high-mass ends of the curves is consistent with Poisson noise from binning the halo masses in order to construct the differential mass function.

Algorithm			b =	Range of	
		0.25	0.2	0.1	$\lg(M/M_{\odot})$
FOF		0.110	0.098	0.505	$13.3 \dots 15.25$
DENMAX,	64^3 grid	1.551	1.565	1.579	$13.3 \dots 15.25$
	96^3 grid	0.840	0.841	0.852	$13.3 \dots 15.25$
	128^3 grid	0.583	0.584	0.591	$13.3 \dots 15.25$
	192^3 grid	0.287	0.288	0.295	$13.3 \dots 15.25$
SKID,	256 neighb.	0.641	0.647	0.663	$14.3 \dots 15.25$
	128 neighb.	1.379	1.389	1.416	$13.8 \dots 15.25$
	64 neighb.	1.838	1.862	1.921	$13.3 \dots 15.25$
	32 neighb.	0.633	0.624	0.620	$13.3 \dots 15.25$
	16 neighb.	0.221	0.193	0.213	$13.3 \dots 15.25$

Table 2: Goodness of agreement Δ between the differential mass function of halos as determined by several different algorithms and its prediction from Press-Schechter theory, for the simulation and set of parameters which are shown in Fig. 2. The upper and lower limits of the mass range, over which Δ is calculated, are given in the last column. The numbers for SKID with 256 and 128 neighbors are smaller only because the mass range had to be restricted as no small groups were identified in these two cases. Furthermore, because of lack of high-mass halos, Δ with SKID with 16 nearest neighbors and b = 0.1 was calculated for $\lg(M/M_{\odot}) = 13.3...14.9$.

The linking lengths used are b = 0.25, b = 0.2, and b = 0.1, in units of the mean particle separation. These values cover the range used in the literature. We see that the differential mass function obtained with FOF depends strongly upon b, and that the value b = 0.2 gives good agreement with Press-Schechter theory. (This has been noticed earlier in [16] and [17] — see [18] for a comparison of FOF with virialized halos.) For FOF, the different values of the linking length effectively correspond to different values of the density contours, inside which particles are grouped together, and therefore we expect a strong dependence upon that parameter. Since FOF does not require the calculation of particle densities, b is the only free parameter for this algorithm. In contrast, DENMAX and SKID show hardly any variation with the linking length. This is not surprising. During the first phase of these two algorithms the particles are moved towards the closest density maximum until their locations vary by less than the convergence radius. But the linking length of the FOF step during the second phase is twice the convergence radius. Hence changing balso changes how tight the moved particles cluster around the density maxima. But the location of the density maxima is independent of the linking length, and so the FOF step scoops up the same particles into the same groups before the removal of gravitationally unbound particles takes place, which is based upon the original, unmoved locations.

Instead, DENMAX and SKID show a strong dependence upon the resolution at which the density

gradients are calculated. (The resolution of the simulation stays the same throughout this discussion as the number of particles is kept the same.) For DEN-MAX, the grid size was increased from 64^3 (the same as the number of particles) to 192^3 (the largest size handled by the workstation on which the calculations were performed). For SKID, the number of nearest neighbors was reduced from 256 to 16. It can be seen from Fig. 2 that a low resolution of the density field (corresponding to a small grid or a large number of neighbors) produces preferably large halos, since there are few density maxima present inside the volume towards which all of the particles are moved. Each of the density maxima will then end up with a large number of particles, and hence larger groups are produced. On the other hand, with high resolution of the density field (i.e. large grids or small number of neighbors), it becomes bumpy, and, except for the densest regions, each particle will correspond to a density maximum at its location. Thus the particles will not move much during the first phase of DENMAX and SKID, and these algorithms become close to plain FOF. This can be seen clearly in Fig. 2 where the curves for DENMAX and SKID come closer to the Press-Schechter prediction (to which FOF with b = 0.2 is very close as seen above) as the resolution of the density field increases. We also see an emergence of variation in the differential mass function with the linking length for the high resolution version of SKID with 16 neighbors, as we would expect if this algorithm became more similar to FOF.

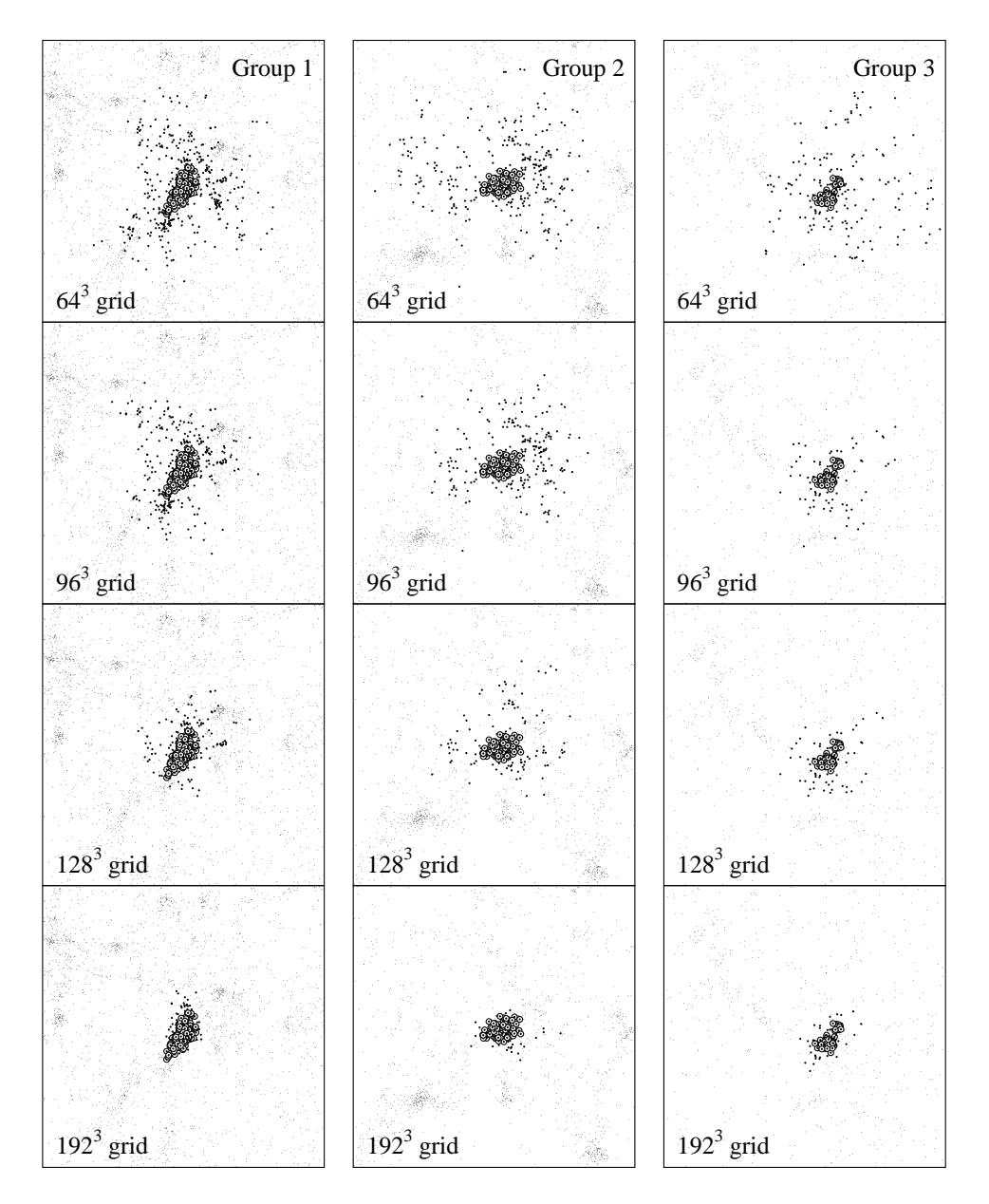


Figure 3: Three representative groups from the 400 Mpc OCDM simulation, as identified by DENMAX and FOF, both with linking length b=0.2, but different grid resolution in the calculation of the density gradients for DENMAX. Particles, which are members of the corresponding DENMAX group, are marked by filled circles, while those in the FOF groups are marked by additional open circles. Particles, which do not belong to the DENMAX groups, are shown as dots. The left panel (for group 1) shows a $(70 \text{ Mpc})^3$ cube, the central and right one (for groups 2 and 3) a $(50 \text{ Mpc})^3$ cube, each projected along the z axis of the simulation.

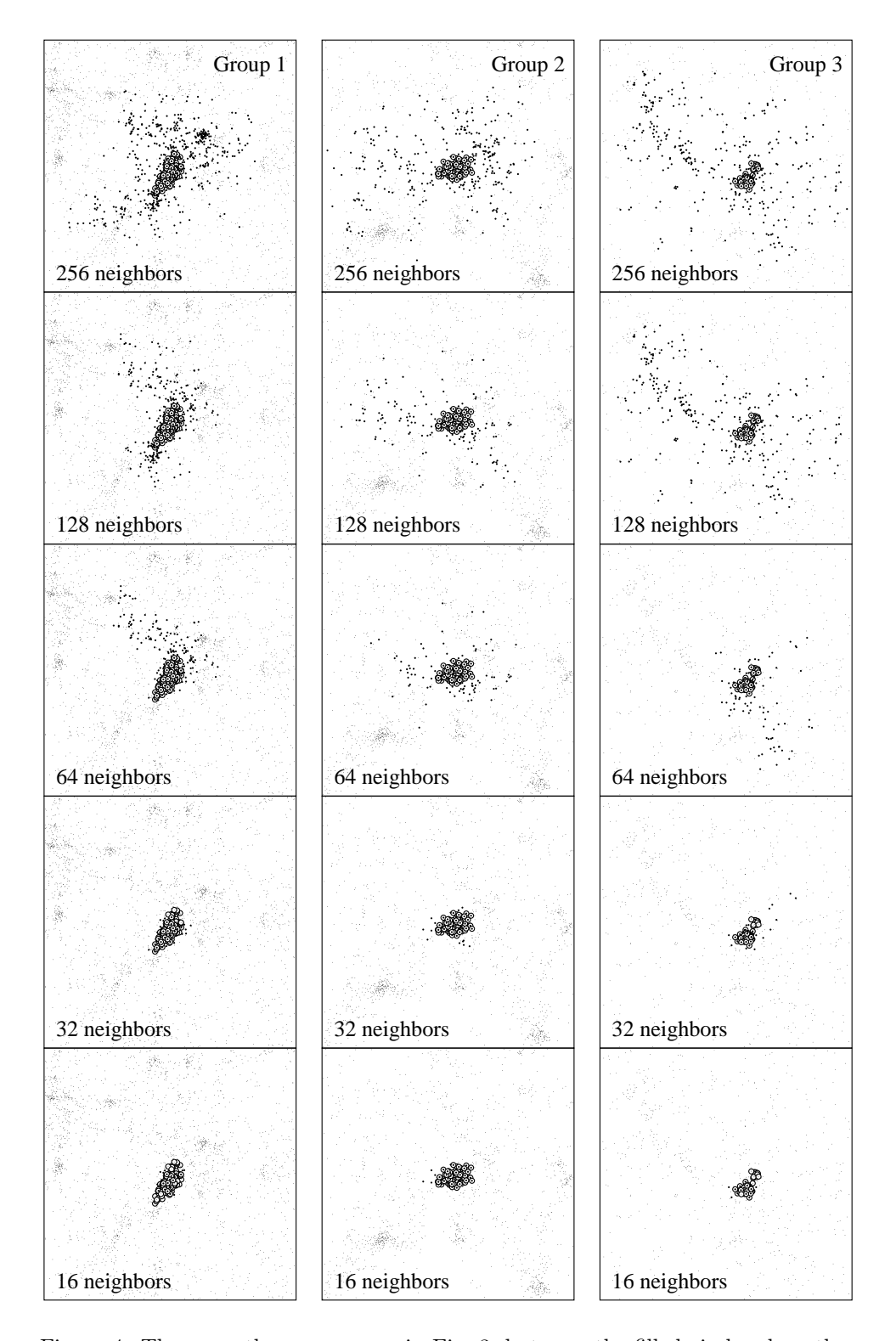


Figure 4: The same three groups as in Fig. 3, but now the filled circles show the groups as identified with SKID at different resolutions of the density field (with b = 0.2).

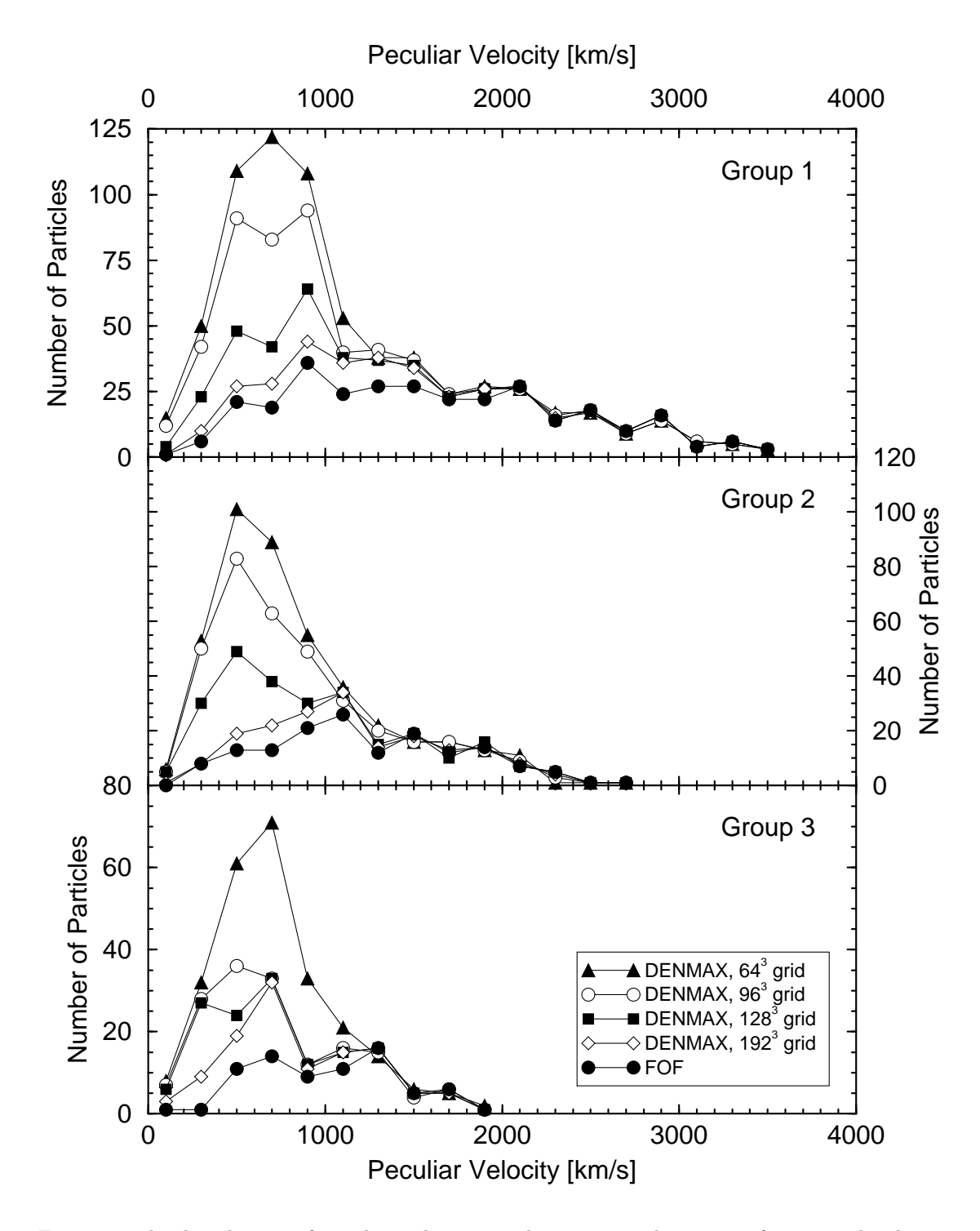


Figure 5: The distribution of peculiar velocities with respect to the center of mass in the three groups from Fig. 3 for FOF and the different resolutions of DENMAX (with b=0.2). The peculiar velocities contain a component from the Hubble expansion of the group.

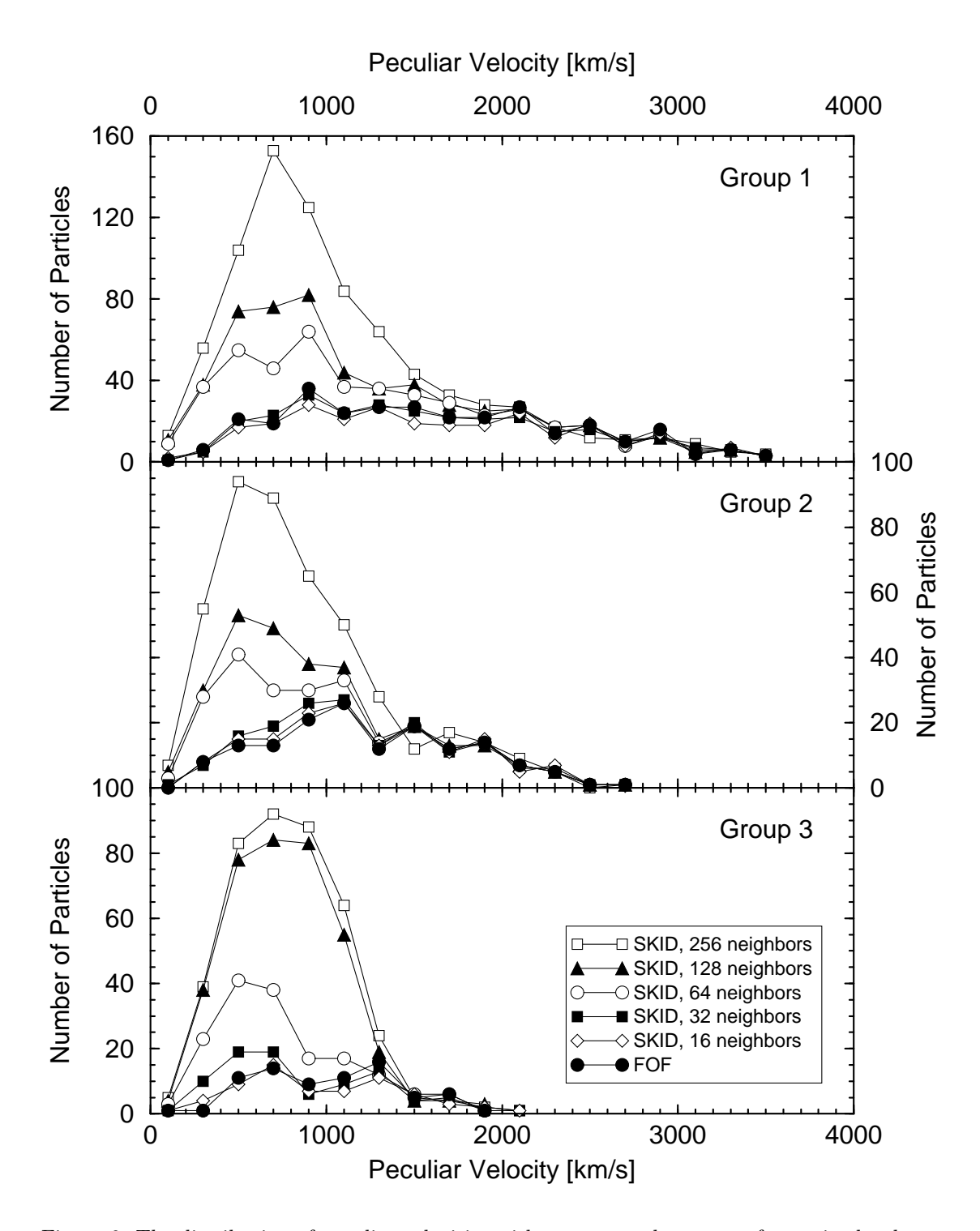


Figure 6: The distribution of peculiar velocities with respect to the center of mass in the three groups from Fig. 4 for FOF and the different resolutions of SKID (with b=0.2). The peculiar velocities contain a component from the Hubble expansion of the group.

Algorithm		Group 1		Group 2		Group 3	
		# of	$\sigma_{ m 1D}$	# of	$\sigma_{ m 1D}$	# of	$\sigma_{ m 1D}$
		part.	[km/s]	part.	$[\mathrm{km/s}]$	part.	[km/s]
FOF		303	1037	152	781	75	626
DENMAX,	64^3 grid	681	768	421	561	253	462
	96^3 grid	587	811	360	579	158	486
	128^3 grid	438	910	260	642	144	502
	192^3 grid	365	981	184	739	116	548
SKID,	256 neighb.	800	753	446	566	407	489
	128 neighb.	549	834	286	629	372	485
	64 neighb.	466	882	238	663	164	491
	32 neighb.	293	1031	168	757	88	563
	16 neighb.	265	1052	159	770	66	620

Table 3: The number of particles and the 1D velocity dispersions σ_{1D} (averaged over all possible lines of sights) for the three groups in Figs. 3 through 6 as identified by the different group finding algorithms (all have b = 0.2).

Table 2 summarizes these results in numeric form. FOF with b=0.2 has the overall smallest value of the goodness of agreement Δ . This is the case even when compared to those values for SKID, where a smaller mass range for Δ had to be used because of the lack of groups at the low-mass or high-mass ends. The values of Δ in Table 2 for SKID with 256, 128, and 16 neighbors (there for b=0.1 only) are only lower limits because of the restricted mass ranges. For DENMAX and SKID we see, at the same grid size or number of neighbors, very little variation of Δ with the linking length, but an improvement towards the values obtained with FOF as the resolution is increased.

To see more clearly where the large halos in lowresolution DENMAX and SKID originate we have isolated three typical halos in the 400 Mpc OCDM simulation, confining ourselves to a linking length of b = 0.2 for the moment. Figs. 3 and 4 compare the group identifications of FOF with those of DENMAX and SKID, respectively. We see that lowresolution DENMAX and SKID indeed produce very extended halos, as argued above from the smaller number of density maxima in the simulation volume. The gravitational unbinding step in both algorithms does not seem to be able get rid of all of these outlying particles, which based upon the visual appearance should not be regarded as members of the halo. As can be seen from Figs. 5 and 6, it retains particles which have a low peculiar velocity with respect to the center of mass of the halo in these outlying regions. There is no shortage of such particles, as we expect the particles in these regions to have low peculiar velocities due to the shallow potential there. The situation improves for the higher resolution versions of DENMAX and SKID when these outlying particles are not considered to be group members in the first place because these two algorithms become closer to plain FOF.

The inclusion of outlying particles with low peculiar velocities in low-resolution DENMAX and SKID biases the velocity dispersion to lower values in these cases, as can be seen in Table 3. Thus the choice of group identification not only affects the masses of the halos, but also actual physical observables like the 1D velocity dispersion of a halo.

The same results are observed in the 400 Mpc box of the SCDM simulation.

5.2. Varying the Box Size

To compare the group finding algorithms at different resolutions of the simulations we looked at different box sizes (since the number of dark matter particles is kept the same). The best values for the parameters found in the discussion above are used, i.e. b=0.2 for the linking length of FOF and the highest resolution in calculating the density field for DENMAX and SKID. Since the choice of b for DENMAX and SKID does not make much of a difference, the same value b=0.2 was chosen for these two algorithms.

The resulting differential mass functions are plotted in Fig. 7 for the OCDM Hydra simulations, and in Fig. 8 for the SCDM Hydra simulations. At visual inspection, the three algorithms seem to perform equally up to box sizes of 200 Mpc (for OCDM) and 400 Mpc (for SCDM), above which DENMAX and SKID start again to produce a larger number of massive halos as compared with FOF or Press-Schechter theory. At the low-mass ends, FOF and

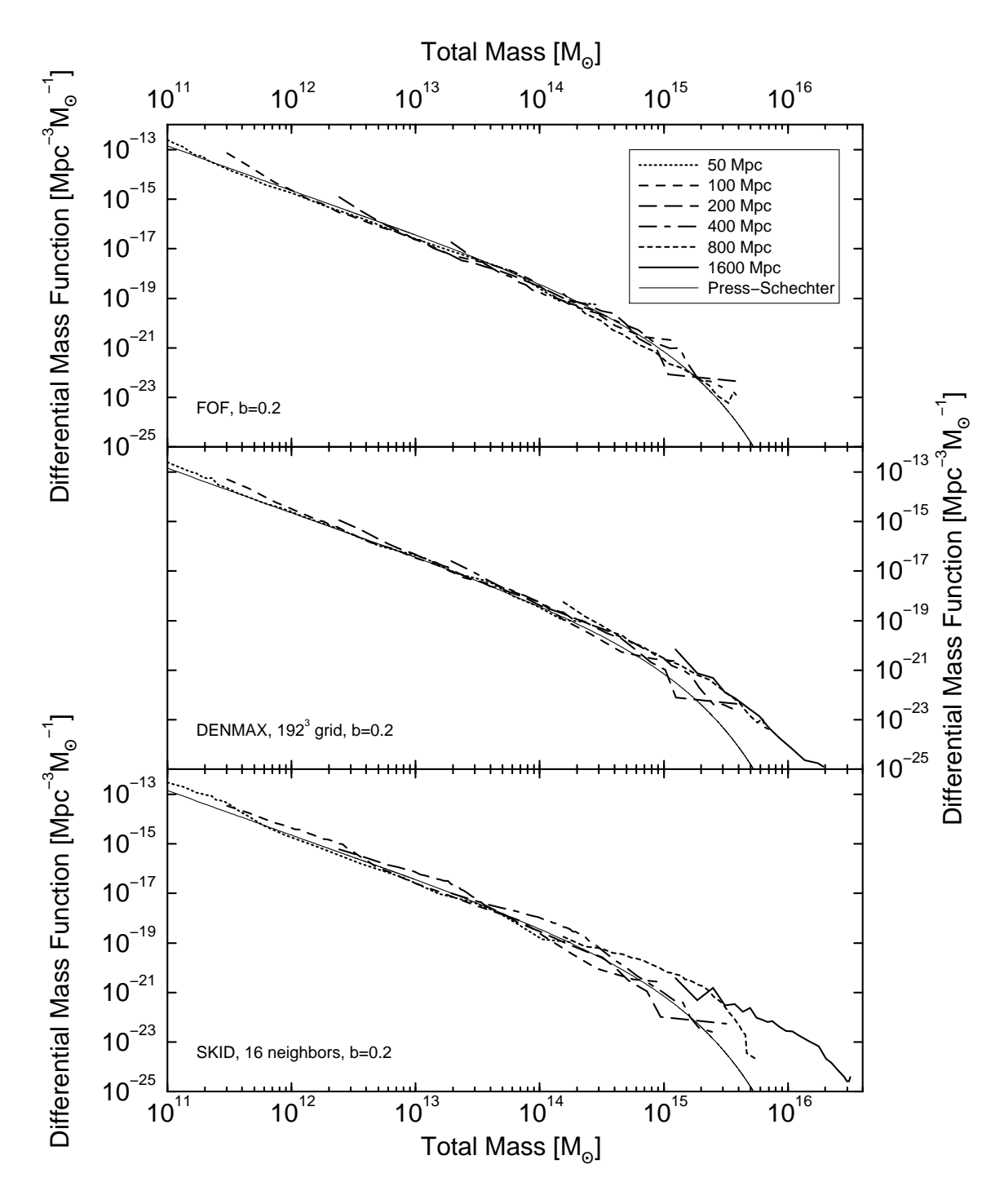


Figure 7: The differential mass functions at redshift z=0 for the OCDM Hydra simulation ($\Omega_0=0.4$, h=0.6) with 64^3 dark matter particles and box sizes varying from 50 Mpc to 1600 Mpc. FOF was run with linking length b=0.2 (in units of the mean particle separation), and DENMAX and SKID with the same b and the highest resolution for calculating the density field, i.e. a 192^3 grid or 16 neighbors, respectively. For the 1600 Mpc box, FOF produced too few groups to successfully construct a reliable differential mass function, which is thus missing from the plot. The scatter at the high-mass end is consistent with Poisson noise.

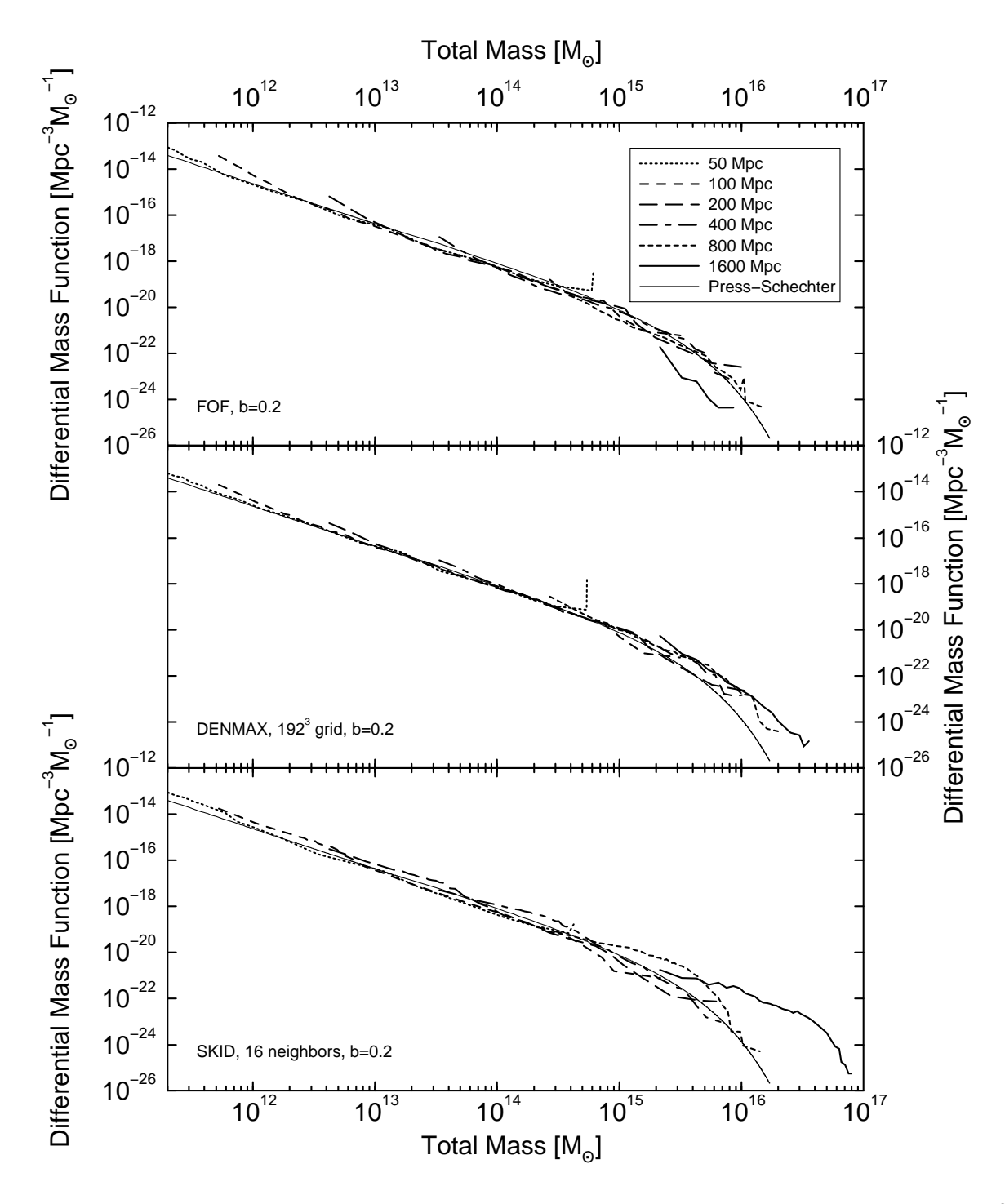


Figure 8: The same as Fig. 7, but now for the SCDM Hydra simulations ($\Omega_0 = 1$, h = 0.5) with 64^3 dark matter particles. With the 1600 Mpc box, FOF again produced very few groups. Although a nominal differential mass function was determined and is shown in this plot, it is not reliable and will not be used in the further discussions.

Algorithm	Box size in Mpc				
	50	100	200	400	800
FOF, $b = 0.2$	0.038	0.068	0.149	0.101	0.063
DENMAX, 192^3 grid, $b = 0.2$	0.023	0.037	0.094	0.307	0.494
SKID, 16 neighbors, $b = 0.2$	0.118	0.186	0.238	0.191	1.119
Range of	11.0	11.9	12.8	13.7	14.6
$\lg(M/M_{\odot})$	14.0	14.9	15.4	15.4	15.4

Table 4: Goodness of agreement Δ between the differential mass function of halos as determined by several different algorithms and its prediction from Press-Schechter theory, for the OCDM simulations which are shown in Fig. 7. The upper and lower limits of the mass range, over which Δ is calculated, are given in the last two rows.

Algorithm	Box size in Mpc				
	50	100	200	400	800
FOF, $b = 0.2$	0.066	0.089	0.126	0.094	0.093
DENMAX, 192^3 grid, $b = 0.2$	0.025	0.028	0.023	0.090	0.382
SKID, 16 neighbors, $b = 0.2$	0.126	0.245	0.214	0.081	0.573
Range of	11.3	12.2	13.1	14.0	14.9
$\lg(M/M_{\odot})$	14.3	15.2	15.7	15.7	16.0

Table 5: Goodness of agreement Δ between the differential mass function of halos as determined by several different algorithms and its prediction from Press-Schechter theory, for the SCDM simulations which are shown in Fig. 8. The upper and lower limits of the mass range, over which Δ is calculated, are given in the last two rows.

DENMAX show an overabundance with respect to Press-Schechter theory. But the smallest groups plotted in Figs. 7 and 8 consist of only two particles, and hence this overabundance is not worrisome as such small groups would be neglected in real applications anyhow.

The goodness of agreement Δ with Press-Schechter theory, calculated over a mass range which excludes these smallest groups, confirms the trend in the plots. For the OCDM Hydra simulations, Table 4 shows that actually DENMAX has the best agreement up to 200 Mpc, after which FOF fares the best. SKID is always worse than FOF and, except for one case, even DENMAX. Similarly, Table 5 for the SCDM Hydra simulations prefers DENMAX up to 200 Mpc, SKID slightly for 400 Mpc, and FOF for 800 Mpc, when compared with Press-Schechter theory. For the 1600 Mpc simulations, FOF produced a very small number of halos, such that it was not possible to construct a reliable mass function in the OCDM model, and only a very unreliable one in the SCDM model. Therefore, the 1600 Mpc box has been omitted from the comparison in Tables 4 and

6. Conclusions

The most basic property of a dark matter halo, its mass, depends upon the choice of group finding algorithm and its free parameters. Many of the other properties are likely to do so as well, and we have shown circumstantial evidence of this for the velocity dispersion. Much care has to be taken in choosing the right algorithm for the purpose in question. If the task is to reproduce the mass distribution as predicted by Press-Schechter theory (which might not be correct, though), the popular DEN-MAX and SKID algorithms have to be run with a very high resolution of the density field. DENMAX this means a large grid (larger than the number of particles), and for SKID a small number of neighbors (smaller than 64 neighbors, which is the default number recommended by the authors of SKID [8]). Under these circumstances, DEN-MAX and SKID become close to a simple FOF algorithm, which, for the right linking length, generally gives the best agreement with Press-Schechter theory and at a much smaller computational cost. Similar effects are seen when instead of the resolution of the algorithm the resolution of the simulation is changed. With fixed number of particles, DENMAX and SKID perform worse, with respect to Press-Schechter theory, as the box size is increased, with FOF faring better. These results hold up for both cosmological scenarios studied.

In cases with low resolution, DENMAX and SKID produce more massive halos as compared with Press-Schechter theory and FOF. These halos are larger because DENMAX and SKID have the tendency of including distant particles which have a low peculiar velocity, a problem from which FOF does not seem to suffer. This would make FOF the preferable algorithm, and imply with its close agreement with Press-Schechter theory, that its predictions are doing quite well, too.

Acknowledgments

We wish to thank Edmund Bertschinger for providing the P³M code, and Hugh Couchman and the Hydra Consortium and the University of Washington group of the High Performance Computing and Communication Program for making the N-body simulation and group identification codes available to the cosmology community on the World Wide Web. Further thanks go to Lars Hernquist, Ue-Li Pen, and David Weinberg for discussions and comments on a first draft of this paper. Part of the computational work in support of this research was performed at the Theoretical Physics Computing Facility at Brown University. MG is supported by an SAO Predoctoral Fellowship and a Manning Fellowship from Brown University.

References

- [1] E. Bertschinger and J. M. Gelb, *Computers in Physics* 5, 164 (1991).
- [2] H. M. P. Couchman, P. A. Thomas, and F. R. Pearce, Astroph. J. 452, 797 (1995).
- [3] U.-L. Pen, Astroph. J. 498, 60 (1998).
- [4] V. R. Eke, S. Cole, and C. S. Frenk, Mon. Not. R. Astron. Soc. 282, 263 (1996).
- [5] J. P. Huchra and M. J. Geller, Astroph. J. 257, 423 (1982).
- [6] M. Davis, G. Efstathiou, C. S. Frenk, and S. D. M. White, Astroph. J. 292, 371 (1985).
- [7] J. M. Gelb and E. Bertschinger, Astroph. J. 436, 467 (1994).
- [8] J. Stadel, N. Katz, D. H. Weinberg, and L. Hernquist, http://www-hpcc.astro.washington. edu/tools/SKID (1997).

- [9] D. H. Weinberg, L. Hernquist, and N. Katz, Astroph. J. 477, 8 (1997).
- [10] R. W. Hockney and J. W. Eastwood, Computer Simulation Using Particles, IOP Publishing, Bristol (1988).
- [11] L. Hernquist and N. Katz, Astroph. J. Suppl. 70, 419 (1989).
- [12] W. H. Press and P. Schechter, Astroph. J. 187, 425 (1974).
- [13] J. R. Bond, S. Cole, G. Efstathiou, and N. Kaiser, Astroph. J. 379, 440 (1991).
- [14] C. Lacey and S. Cole, Mon. Not. R. Astron. Soc. 262, 627 (1993).
- [15] M. A. K. Gross *et al.*, astro-ph/9712142 (1997).
- [16] G. Efstathiou, C. S. Frenk, S. D. M. White, and M. Davis Mon. Not. R. Astron. Soc. 235, 715 (1988).
- [17] C. Lacey and S. Cole, Mon. Not. R. Astron. Soc. 271, 676 (1994).
- [18] S. Cole and C. Lacey, Mon. Not. R. Astron. Soc. 281, 716 (1996).